Kinetics of Light-dependent Ca Fluxes across the Plasma Membrane of Rod Outer Segments

A Dynamic Model of the Regulation of the Cytoplasmic Ca Concentration

DONALD L. MILLER and JUAN I. KORENBROT

From the Departments of Physiology and Biochemistry, University of California Medical School, San Francisco, California 94143

ABSTRACT We measured simultaneously in single toad rods the membrane photocurrent and the Ca concentration in a small volume surrounding the outer segment. Illumination causes a rise in the extracellular Ca concentration. Photocurrents and Ca concentration changes occur over the same range of light intensities. Analysis of the time course of the Ca concentration changes suggests that these concentration changes arise from the difference in the transport rates of light-activated Ca influx and efflux across the outer segment plasma membrane. The Ca influx occurs through the light-sensitive channels of the outer segment membrane and the efflux through Na/Ca exchangers. In 0.1 mM external Ca, ~1–2% of the dark current is carried by Ca ions. The Ca efflux in the dark is identical to the influx, $\sim 2 \times 10^6$ ions/s. Upon illumination, the Ca influx decreases with a time course and light sensitivity identical to those of the photocurrent. The Ca efflux, on the other hand, has very different kinetics from those of the photocurrent. Upon illumination, the Ca efflux decreases with a time course and light sensitivity determined by the change in membrane voltage and in the free cytoplasmic Ca concentration near the plasma membrane. In response to bright stimuli, which saturate the photocurrent for prolonged periods of time, the Ca efflux decays with an exponential time course from its value in darkness. The average time constant of this decay is 2.5 s. From the kinetics of the light-activated Ca fluxes, it is possible to predict that illumination causes a decrease in the cytoplasmic Ca concentration. We present a model of the regulation of the cytoplasmic Ca concentration by the dynamic balance of the Ca influx and efflux from the rod outer segment. The model accounts for our experimental observations and allows us to predict the time course and extent of the light-dependent decrease in the free cytoplasmic concentration.

Address reprint requests to Dr. Donald L. Miller, Dept. of Physiology, University of California Medical School, San Francisco, CA 94143.

J. GEN. PHYSIOL. © The Rockefeller University Press · 0022-1295/87/09/0397/29 $2.00

Volume 90 September 1987 397–425

INTRODUCTION

Rod photoreceptors in the vertebrate retina respond to illumination with a photocurrent whose amplitude and time course are defined by the stimulus intensity (Hagins et al., 1970; Penn and Hagins, 1972; Baylor et al., 1979). The photocurrent is generated by the closure of ionic channels in the plasma membrane of the rod outer segment (Bodoia and Detwiler, 1985; Haynes et al., 1986; Zimmerman and Baylor, 1986). Elegant experiments have demonstrated that changes in the cyclic GMP concentration can control the opening of the light-sensitive channels of the outer segment membrane (Fesenko et al., 1985; Matthews et al., 1985; Cobbs and Pugh, 1985; Zimmerman and Baylor, 1986; Haynes et al., 1986). However, it is unlikely that the regulation of the photocurrent amplitude and time course is an exclusive function of the changes in the cyclic GMP concentration since intracellular Ca buffers have pronounced effects on the photosensitivity and kinetics of the photocurrent (Matthews et al., 1985; Lamb et al., 1986; Korenbrot et al., 1986; Korenbrot and Miller, 1986). Also, illumination of intact rods causes a Ca efflux that is sufficiently large and rapid to suggest a role in phototransduction (Gold and Korenbrot, 1980, 1981; Yoshikami et al., 1980).

The light-dependent Ca efflux from the outer segment is mediated by Na/Ca exchangers present in the plasma membrane and results in an increase in the Ca concentration in the space surrounding the outer segment (Gold and Korenbrot, 1980, 1981; Yoshikami et al., 1980). The Ca efflux was originally interpreted to be a consequence of the activation of the Na/Ca exchangers by a light-dependent increase in the cytoplasmic free Ca concentration (Yoshikami et al., 1980; Gold and Korenbrot, 1981). MacLeish et al. (1984) challenged this interpretation on the basis of the subsequent, and surprising, discovery that the light-sensitive channels of the outer segment are permeable to Ca (Yau and Nakatani, 1984; Hodgkin et al., 1985). An alternative model to explain the light-dependent Ca concentration change was detailed by Yau and Nakatani (1985) and tested by Gold (1986). In their model, Yau and Nakatani proposed that in the dark there exists a kinetic balance between Ca influx, via the light-sensitive ionic channels, and Ca efflux, via Na/Ca exchangers. Illumination reduces both fluxes, but the Ca efflux decelerates more slowly than the Ca influx. This imbalance in flux rates results in the observed net Ca efflux, followed by a net Ca influx necessary to restore the initial conditions. Measurement of the kinetics of the light-dependent Ca flux across the outer segment membrane and its resolution into influx and efflux components should allow insight into the adequacy of the two alternative models discussed above and into the role of Ca in the mechanism of phototransduction.

We describe in this article the simultaneous measurement of photocurrent and light-dependent Ca release by the outer segment of intact single toad rods. We present an experimental method that resolves the net Ca flux across the outer segment membrane into its influx and efflux components and we compare the kinetics of these components with those of the photocurrent. Our experimental data lead us to develop a dynamic model of the plasma membrane mechanisms that control the cytoplasmic Ca concentration in the outer segment. This model

predicts light-dependent decrements in the cytoplasmic Ca concentration, whose time course and extent can be estimated. A brief account of this research has appeared (Korenbrot and Miller, 1986).

MATERIALS AND METHODS

Materials

Marine toads, *Bufo marinus*, were maintained under running water at 24°C under 12-h dark-light cycles. They were fed meal worms ad lib once a week. The Ca salts of bis(di-*n*-octyl)phenyl phosphate (HDOPP) and di-octylphenyl phosphonate (DOPP) were purchased from Specialty Organics (Irwindale, CA). Tetrahydrofuran (THF) and polyvinylchloride (PVC; high molecular weight) were obtained from Aldrich Chemical Co. (St. Louis, MO). Na-tetraphenylboron was obtained from Sigma Chemical Co. (St. Louis, MO). Tetraethylammonium (TEA) and tetramethylammonium (TMA) chloride were purchased from Kodak Chemicals (Rochester, NY). Ortho-nitrophenyloctyl ether (*o*-NPOE), bis(dimethyl-amino)dimethyl-silane, and K-tetrakis-(4-chlorophenyl)-borate were obtained from Fluka, A. G. (Buchs, Switzerland).

Incubation Medium and Retinal Preparation

Dissections and electrical recordings were carried out in modified Leibovitz L-15 medium. Customized L-15 medium, prepared at the University of California, San Francisco, tissue culture facility without Ca and phenol red, was diluted in water to obtain a 35% vol/vol solution. The solution was supplemented to obtain the following final concentrations (millimolar): 108 NaCl, 1 Na_2HPO_4, 3.5 KCl, 0.14 KH_2PO_4, 0.6 $MgCl_2$, 0.6 $MgSO_4$, 0.1 $CaCl_2$, 10 glucose, and 10 HEPES. The solution was adjusted to pH 7.5–7.6; its osmotic pressure was 255–258 mosM. To retard microorganism growth, penicillin (100 U/ml) and streptomycin (100 μg/ml) were sometimes added to the solution. Control experiments demonstrated that the addition of these antibiotics did not affect rod phototransduction. The solution was equilibrated with air.

Eyes were enucleated from double-pithed, dark-adapted animals under dim red light. A small square section, 5–8 mm on the side, was cut from the posterior pole of the eye. The retina was removed from this section and mounted flat, photoreceptor side up, on filter paper (HAWP 02500, Millipore/Continental Water Systems, Medford, MA). Under infrared illumination, the retina on the Millipore support was cut in a tissue-chopper along two orthogonal directions at ~50-μm intervals. The resulting suspension of retinal fragments and isolated rod cells was transferred to the recording chamber.

Recording Chamber and Photostimulation

The recording chamber was constructed of black nylon and is illustrated in Fig. 1*A*. The chamber had a volume of 0.35 ml and its glass bottom was silanized by application of 10 μl of amino-silane at room temperature, followed by overnight drying. The bottom was repeatedly silanized as needed. The top of the chamber was a 0.1-mm-thick glass coverslip that was replaced in every experiment. One port on the side of the nylon chamber connected it to a reference electrode through a salt bridge made of 3 M KCl in 2% agar, while the other port allowed the continuous perfusion of the medium in the chamber. The perfusate was gravity-fed and collected by suction through a tube placed in the opening of the chamber. The perfusion rate was ~0.06 ml/min.

The recording chamber was mounted on the stage of an upright microscope. Cells were observed under infrared illumination with the aid of a TV camera and monitor. Images of cells being studied were recorded on a videocassette recorder for later analysis.

Electrodes were mounted on a conically shaped multiport electrode holder, designed by Dr. J. Lisman (Brandeis University, Waltham, MA).

Photoreceptors in the recording chamber were illuminated with 22-ms-duration flashes of unpolarized, diffuse light of 500 nm wavelength. Light was spectrally selected with a

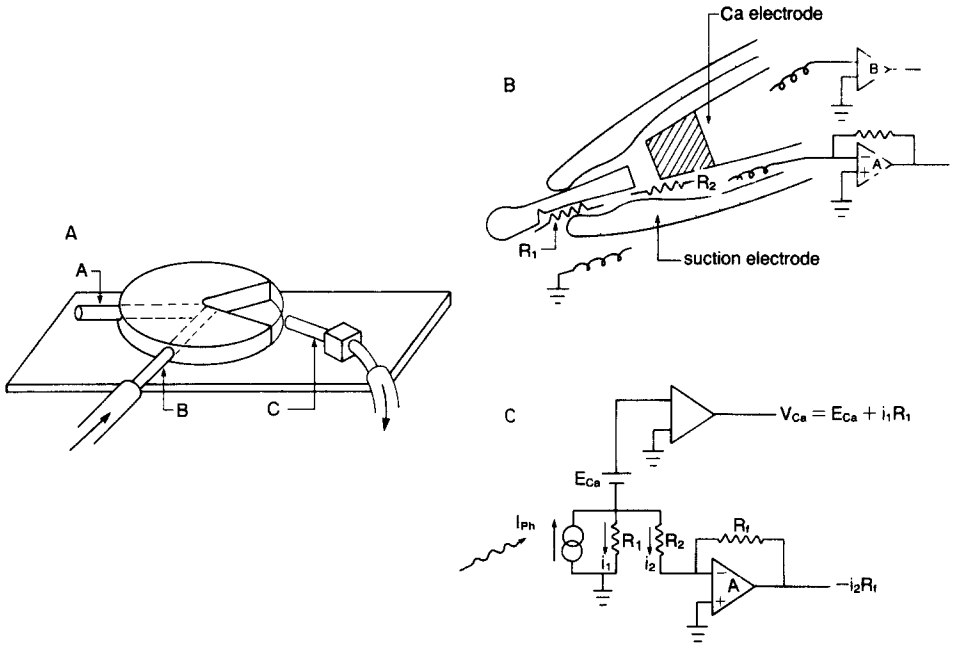

FIGURE 1. Schematic representation of the instruments used to measure simultaneously photocurrents and Ca concentration changes in a single toad rod. Panel *A* illustrates the recording chamber. Electrodes had access to the cells in the chamber through the opening on the right. *A* and *C* are the inlet and outlet, respectively, of a gravity-fed perfusion system that continuously exchanged the bathing medium in the chamber. *B* is the connection port for an agar salt bridge. The bottom of the chamber was a silanized glass slide and the top was a circular coverslip. Panel *B* illustrates the electrode assembly used in the experiments with a rod outer segment in place. Also illustrated are the sites that create significant access resistance in the electrical measurements: R_1, the seal between the outer segment and the suction electrode, and R_2, the seal between the Ca-sensitive and suction electrodes. Panel *C* is an electrical equivalent representation of the measuring circuits. The Ca concentration change generates a voltage, E_{Ca}, in the ion-sensitive electrode that is measured by amplifier *B*. The rod outer segment generates a photocurrent, I_{ph}, that is measured by amplifier *A*. The existence of access resistances R_1 and R_2 generates two potential artifacts in the measurements: (*a*) the photocurrent can divide between the two seal resistances and (*b*) the voltage amplifier *B* can measure, in addition to E_{Ca}, a voltage generated by the flux of photocurrent through resistance R_1. The text describes the methods used to minimize the perturbing effects of these signals in the measurements.

narrow-band interference filter (10 nm half-bandwidth, Ealing Corp., South Natick, MA) and its intensity was controlled with neutral density filters (Melles-Griot, Irvine, CA). The intensity of the light was measured before each experiment with a calibrated photodiode (model UV100, United Detector Technology, Santa Monica, CA) placed on the micro-

scope stage. Light intensity was expressed in units of photoexcited rhodopsin molecules per rod (Rh*) by calculating the effective collecting area of the outer segment for unpolarized light, A (Miller, 1986):

$$A = d^2(l/4)f\pi 2.303\alpha Q(1 + 1/r),$$

where d and l are the outer segment diameter and length, Q is the quantum yield of rhodopsin excitation (0.67; Dartnall, 1972), α is the transverse specific density (0.016; Hárosi, 1975), f is 0.5 for unpolarized light, and r is the dichroic ratio of absorbance (4.06; Hárosi, 1975). The collecting area of a toad rod outer segment illuminated on its side is 33.2 μm^2. Light intensity, in units of photons per square micrometer, can be calculated from our data by considering that, on the average, a single rhodopsin molecule is photoexcited at an intensity of 29.9×10^{-3} photons/μm^2.

Photocurrent Measurement: Suction Electrodes

To measure independently membrane current and Ca flux in the same rod outer segment, a Ca-selective electrode was placed near the outer segment tip within a conventional suction electrode. Suction electrodes were constructed from 1.5 min o.d./1 mm i.d. glass capillary tubing cleaned in aqua regia for 30 min, followed by thorough rinsing with distilled water and overnight drying in vacuo over dessicant at 150°C. The suction electrodes were constructed as described by Baylor et al. (1979) with a tip of nearly constant 10 μm i.d. over a length of ~60 μm (see Fig. 2). It was critical to achieve these dimensions to minimize the volume surrounding the outer segment. Suction electrodes were silanized by placing them within a small bell jar in an oven at 250°C for 45 min and then vaporizing the amino-silane within the jar and baking it in the oven for another 45 min. Silanized suction electrodes were used repeatedly. After an experiment, the electrodes were rinsed with distilled water and occasionally with chromic acid, and then they were dried and stored over desiccant.

The suction electrode was connected through a 3 M KCl/2% wt/vol agar bridge to a calomel electrode (Ingold Electrodes, Inc., Andover, MA). The bath in the recording chamber was grounded through a similar salt bridge and electrode. Current signals were measured with a modified current amplifier (model 427, Keithley Instruments, Inc., Cleveland, OH) and stored on magnetic tape (model 4D, Racal Recorders, Irvine, CA). The recording bandpass was DC to 25 Hz. The resistance of the suction electrode in L-15 medium was 3–6 MΩ. The resistance increased from three- to sevenfold when an outer segment was within the electrode.

Ca Concentration Measurement: Ca Electrodes

Ca-selective electrodes were made by plugging the tip of a glass electrode with a PVC polymer containing a liquid Ca exchanger. Glass capillary tubing, 1.0 mm o.d./0.5 mm i.d., was cleaned as described above and pulled to a fine tip. Under microscopic observation, the electrode tip was broken to a diameter of 11–12 μm (see Fig. 2). Electrodes were silanized as described above. To produce Ca-selective electrodes, the silanized glass pipettes were first backfilled with 0.1 mM $CaCl_2$ and 0.1 M NaCl. Under microscopic observation, their tips were then filled by suction with an ~400-μm-long column of PVC/Ca-sensitive liquid exchanger mixture. The mixture was allowed to polymerize overnight.

The Ca exchanger we used was designed and synthesized by Ruzicka et al. (1973). HDOPP was mixed with DOPP, 1:10 wt/wt, and the mixture was allowed to stand overnight at room temperature. 25.5 mg of the HDOPP/DOPP solution was then mixed with 4.5 mg of PVC and 0.18 mg Na-tetraphenylboron (84.5%/14.9%/0.6% wt/wt/wt, respectively) in 0.33 ml of THF. To produce electrodes reliably, we found it critical to use THF freshly distilled over metallic Na. The liquid exchanger mixture was stirred for

~1 h in a covered container until completely clear. Its volume was then reduced by 75% by evaporating THF under a stream of nitrogen while stirring.

The electrodes responded satisfactorily to changes in Ca activity for ~3 d after their manufacture, if kept dry. Satisfactory sensitivity was defined as a Nernstian behavior with 25–30 mV signal per decade change of Ca activity on a 0.1-mM background. The response time of each electrode was measured in a device consisting of a small Plexiglas block into which the electrode was inserted and through which a stream of Ca calibration solution was forced to flow. The calibration solution could be changed completely within 35 ms

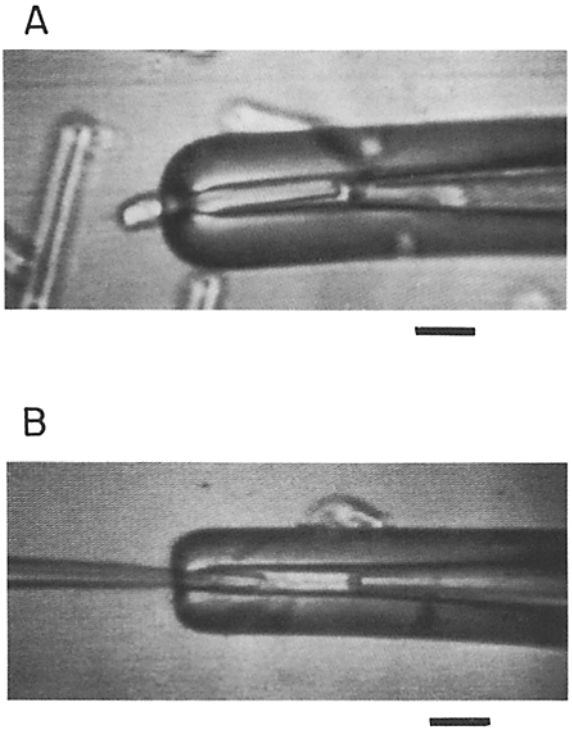

FIGURE 2. Photographs of the electrode assembly taken from a videocassette recording. The assembly consisted of a Ca-sensitive electrode placed within a suction electrode. In *A*, nearly the entire length of the outer segment of an isolated toad rod cell rests within the measuring compartment of the electrode assembly. In *B*, the outer segment is substituted by a double-barreled iontophoresis electrode coated with Sylgard on its outside. The calibration bar is 10 μm.

with the use of electronically activated pneumatic valves. We used only electrodes that responded with a time constant of ≤100 ms to a 10-fold change in Ca activity on a 0.1 mM Ca background. The ion selectivity of the electrodes has been described by Ruzicka et al. (1973).

The Ca electrodes were mounted in electrode holders with built-in Ag/AgCl electrodes (W-P Instruments, Inc., New Haven, CT). The reference for the Ca electrode was the inside of the suction pipette, kept at ground by the current-measuring amplifier (see Fig. 1). The electrode signal was recorded with a high-input-impedance (>10^{13} Ω) amplifier (model 1090, Winston Electronics, San Francisco, CA), further amplified (model 113,

PARC Instruments, Princeton, NJ), low-pass-filtered through an eight-pole Butterworth filter (model 902LPF, Frequency Devices, Inc., Haverhill, MA), and stored on magnetic tape. The overall recording bandpass was DC to 10 Hz. The Ca electrodes measure the Ca ion activity, not its concentration. The data presented in this report are expressed in units of Ca concentration, calculated from the experimentally determined electrode calibration and taking the activity coefficient of Ca in the L-15 medium to be 0.42, as calculated from the Debye-Huckel theory (Amman et al., 1975).

TEA Electrodes

A TEA-sensitive electrode was produced by following the method described above for the Ca electrode, but backfilling the glass pipette with 0.1 mM TEA-Cl and 0.1 M NaCl and using a TEA liquid exchanger. The TEA liquid exchanger was a 3% wt/vol solution of K-tetrakis-(4-chlorophenyl)-borate in *o*-NPOE. This solution was mixed with PVC and THF in the ratio 7.9%/1.4%/90.7% wt/wt/wt. Satisfactory electrodes responded to a 10-fold change in TEA activity on a 1 mM TEA background with a 57–59-mV signal and with a time constant of response of ≤100 ms. The TEA electrodes were responsive to K in the absence of TEA, but in the presence of 1 mM TEA, the electrode sensitivity to K was reduced to 0.52% of that to TEA. K did not affect the sensitivity of the electrode to TEA. The TEA electrodes were not measurably responsive to changes in Na activities.

Suction/Ca Electrode Assembly and Analysis of Potential Electrical Artifacts

To measure the photocurrent and the Ca release simultaneously, an outer segment was first drawn into the suction electrode and the Ca electrode was then advanced within the suction electrode until its tip was within ≤5 μm from the apex of the outer segment (Fig. 2). With an outer segment in place, measurements of the video-recorded images of the electrode assembly (Fig. 2*A*) showed that the extracellular volume limited by the inner wall of the suction pipette and the tip of the Ca electrode was in the range of 2.7 ± 0.2 pl in all experiments.

A schematic diagram of the electrode assembly is illustrated in Fig. 1*B* and its electrical equivalent circuit is shown in Fig. 1*C*. R_1 is the seal resistance between the outer segment and the suction pipette, while R_2 is the seal resistance between the suction and Ca electrodes. The photocurrent generated by the outer segment within the suction pipette, represented by the current generator in Fig. 1*C*, is measured by the current amplifier, *A*. Since the photocurrent is divided across R_1 and R_2, the current measured by *A* may differ from the true photocurrent, depending on the values of R_2 and R_1. Ideally, R_1 should be much larger than R_2. In our design, R_2 must be kept large to minimize diffusional escape of Ca from the electrode assembly. In our experiments, R_1 had a value in the range of 4–16 MΩ and R_2 was adjusted by the position of the Ca electrode within the suction electrode to be <10 MΩ, typically 6 MΩ.

The true photocurrent, I, can be determined from the measured values of R_1, R_2, and i_2:

$$I = i_1 + i_2;$$

$$i_1R_1 = i_2R_2.$$

Therefore,

$$I = i_2(1 + R_2/R_1).$$

This corrected value is used where appropriate in the calculations and data analysis presented in the text. Experimental data illustrated in the figures are, of course, not corrected and will appear abnormally small.

The signal generated by the Ca electrode in the suction/Ca electrode assembly can include, in addition to a true measurement of the Ca concentration, several artifacts: (*a*) voltage artifacts generated by the photocurrent flowing through the seal resistance between the Ca and suction electrodes (R_2 in Fig. 1); (*b*) a response of the Ca electrode to the activity of ions other than Ca; (*c*) contributions to the Ca concentration change of cellular sources and/or sinks of Ca other than the outer segment; and (*d*) volume changes of the outer segment induced by light. All of these potential problems and their resolution are discussed next.

First, the signal measured by the Ca electrode is the sum of the voltage generated by the ion-selective electrode and the voltage generated by the photocurrent flowing across the seal resistance between the Ca and suction electrodes, R_2. The extent of the artifact generated by the photocurrent is directly proportional to the value of R_2. However, this resistance cannot be made too small because Ca ions would readily escape from the measuring compartment of the electrode assembly. Using an electrode similar in dimension to the Ca electrode, but filled with agar at its tip, we determined that the photocurrent-generated signal in the Ca electrode was detectable only when R_2 was >10 MΩ. Therefore, we measured R_2 in each experiment and kept it at a value of <10 MΩ, typically 6 MΩ.

The second possible artifact does not pose a problem in these experiments, given the ion selectivity of the electrodes (Ruzicka et al., 1973) and the finding that Ca buffers added to the extracellular medium quantitatively attenuate the Ca electrode signal produced by rods, as predicted by their buffering power (Gold and Korenbrot, 1981).

The problem of the cellular source of the Ca signal is resolved by the design of the electrode assembly. Contamination of the Ca electrode signal by cellular sources other than the outer segment is unlikely since the flow of Ca out of (or into) the measuring compartment in the assembly is slow: the time constant of Ca clearance from the electrode assembly is 28.5 ± 6.5 s (see Results). The signals recorded from isolated rods were identical to those recorded from rods embedded in retinal pieces, which indicates that only the rod inner segment, and no other structure in the retina, need be considered as a potential alternative source and/or sink of Ca in our measurements. We ruled out that the inner segment is a light-dependent source or sink of Ca by replacing the outer segment in the electrode assembly by an inner segment. Upon illumination, no discernible changes in Ca concentration around the inner segment were detected, although normal (but inverted) photocurrents were recorded. This is not surprising, although isolated rods exhibit voltage-activated Ca currents (Bader et al., 1982), because these currents are small in the dark (<1 pA) and are distributed throughout the membrane of the inner segment and synaptic terminals. The isolated rods studied here lacked a significant portion of their inner segment and all their synaptic terminals (Fig. 2). Their Ca currents, therefore, are expected to be extremely small. In addition, the current-voltage characteristics indicate that the Ca currents are nearly inactive in the dark and are suppressed by the hyperpolarizing photovoltage (Bader et al., 1982).

Finally, the geometry of the electrode assembly suggests the possibility that changes in the volume of the outer segment upon illumination might appear as changes in extracellular Ca activity as water flows into or out of the cell (Dr. J. Coles, personal communication). We tested this possibility by attempting to measure light-dependent changes in the extracellular concentration of a membrane-impermeant cation, TEA, added to the medium. The concentration of TEA was measured in the presence of an outer segment in a suction/ion-selective electrode assembly in which a TEA-selective electrode replaced the Ca electrode. The TEA electrode exhibited no response, even at the highest level of illumination tested, while the rod photocurrent was entirely normal (data not shown). Thus, the rod outer segment volume does not change sufficiently to generate an artifactual signal in the Ca electrode.

Iontophoresis in the Suction/Ca Electrode Assembly

Ca was injected into the measuring compartment of a suction/Ca electrode assembly by placing a double-barreled electrophoresis electrode within the electrode assembly in the position normally occupied by the outer segment (see Fig. 2). Iontophoresis electrodes were made from theta-glass capillary tubing pulled to a tip ~3 μm in diameter. The electrodes were coated on the outside near their tip with a thin film of Sylgard. The electrophoresis electrode was driven into the electrode assembly until the seal resistance between it and the suction electrode (equivalent to R_1 in Fig. 1) was comparable in magnitude to that obtained between the outer segment and the suction electrode. One barrel of the electrode was filled with 1.0 mM $CaCl_2$ (anode) and the other with 0.1 M NaCl and 0.1 mM $CaCl_2$ (cathode). Ag/AgCl wires were placed in each of the barrels and were connected to the output of a voltage-controlled, constant-current source (model BSI-1, BAK Electronics, Inc., Rockville, MD). Injected currents ranged in magnitude from 1 to 20 nA.

Data Analysis and Computer Modeling

Data were digitized and analyzed offline with a microcomputer (Superscope, R. C. Electronics, Inc., Santa Barbara, CA). Dynamic computer modeling was carried out using block diagram modeling methods (Korn and Wait, 1978) with the aid of a program named TUTSIM (Applied i, Palo Alto, CA) on an IBM-XT computer. This program allows the numerical solution of systems of ordinary differential equations.

RESULTS

Simultaneous Measurement of Photocurrents and Light-dependent Ca Release in a Single Rod

We simultaneously measured the membrane photocurrent and the Ca concentration in single toad rods in a volume of ~2.7 pl surrounding the outer segment. Fig. 3 illustrates typical signals recorded in response to light flashes of varying intensity from an isolated rod in a medium containing 0.1 mM Ca. The isolated rod (Fig. 2) lacked its synaptic end. Essentially identical data were obtained from intact rods still embedded in small retinal pieces. In our analysis, we did not distinguish data obtained from isolated rods from those collected from rods in retinal pieces. The photocurrent time course we observed is similar to that first described by Baylor et al. (1979). The photocurrent peak amplitude increased with light intensity up to a saturating value (see Fig. 10). Further increments in light intensity prolonged the duration of the saturated phase of the photocurrent. We consistently observed a small undershoot in the photocurrent in response to bright flashes after its recovery from saturation.

The data illustrated in Fig. 3 and all data analyzed in this report were collected under a strict experimental protocol designed to minimize artifacts in the Ca electrode signal as discussed in Materials and Methods. Under these conditions, the Ca electrode signals reflect a light-dependent increase in the Ca activity in the small volume surrounding the rod outer segment. The peak amplitude and the initial rate of rise of the concentration increased with light intensity up to a saturating value (see Fig. 10). In response to bright light flashes that saturated the photocurrent for a prolonged period of time, the Ca concentration rise approached a limiting value. The concentration began to decline only as the

photocurrent began to recover from saturation. The concentration changes arose specifically from light-dependent changes in the Ca influx and efflux across the outer segment plasma membrane.

Analysis of the Kinetics of the Membrane Ca Fluxes Underlying the Light-dependent Ca Concentration Change

We propose to develop a model of the Ca fluxes across the outer segment membrane that accounts for the observed light-dependent changes in the extracellular Ca concentration. The observed Ca concentration change, $\Delta[Ca]_o$, is the integral over time of the net Ca flux into the measuring compartment of the

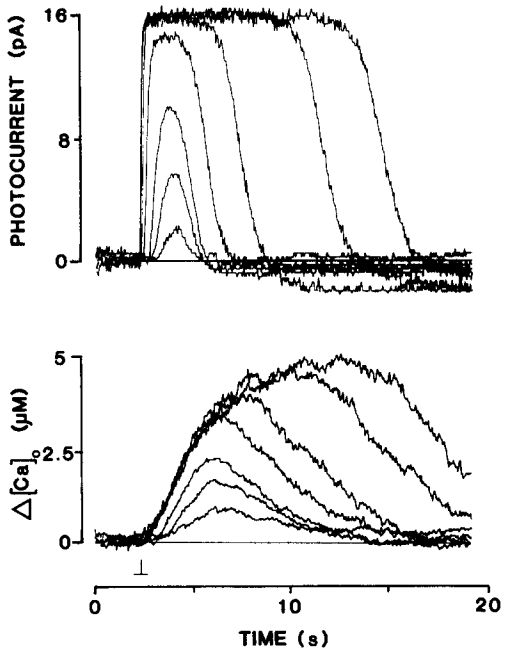

FIGURE 3. Photocurrents and light-dependent increments in extracellular Ca concentration measured simultaneously in a single rod outer segment. The cell was illuminated with 22-ms flashes that excited, on the average, 10, 16, 36, 149, 824, 9,700, and 35,600 rhodopsin molecules. For the three dimmest flashes, eight responses were signal-averaged. The Ca concentration rises from an initial value of 0.1 mM.

electrode assembly used to carry out these measurements (Figs. 1 and 2). This net flux, $J_{net}(t)$, is the algebraic sum of the Ca efflux from the outer segment, $J_e(t)$, the Ca influx into the outer segment, $J_i(t)$, and the Ca efflux from the measuring compartment to the volume outside the electrode assembly, $J_l(t)$. We neglect any Ca influx into the measuring compartment because there is no driving force for such flux. We define the flux into the measuring compartment as positive. Thus,

$$J_{net}(t) = J_e(t) + J_i(t) + J_l(t) \tag{1}$$

and

$$\Delta[Ca]_o = \int J_{net}(t)dt. \tag{2}$$

Next we describe the procedures we used to resolve each of the Ca fluxes that contribute to the Ca electrode signal.

Ca Flux from the Measuring Compartment in the Electrode Assembly to the Surrounding Medium: $J_l(t)$

To determine $J_l(t)$, we measured the clearance rate of Ca iontophoretically injected into the measuring compartment of the electrode assembly. In these experiments, the outer segment in the electrode assembly was substituted by a Sylgard-coated double-barreled iontophoresis electrode (Fig. 2) placed so that the resistance between the suction and iontophoresis electrodes was in the same range of values as that obtained between the suction electrodes and the outer segment. Fig. 4 illustrates typical Ca concentration changes in response to a 2-nA step injection of current. At current onset, the Ca concentration within the measuring compartment rose exponentially until a steady state value was reached.

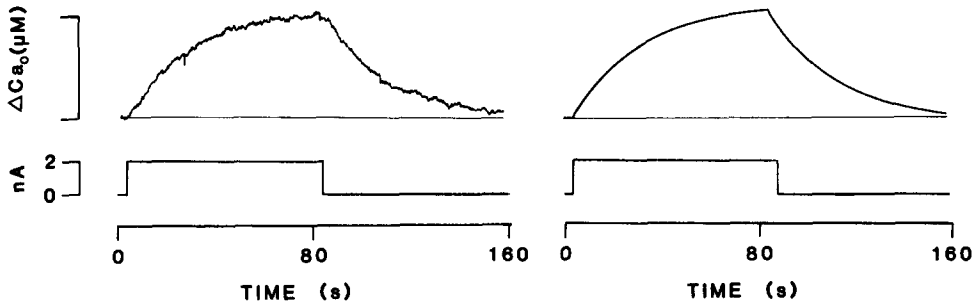

FIGURE 4. Analysis of the Ca leak from the measuring compartment of the electrode assembly. The left-hand panel illustrates experimental data obtained by injecting Ca into the measuring compartment with an iontophoresis electrode. The rise in Ca concentration was measured by the Ca electrode. The injection pulse lasted 80 s and was 2 nA in amplitude. The total seal resistance of the electrode assembly ($R_1 + R_2$) was 20 MΩ, a value comparable to that recorded in experiments with rod outer segments. The right-hand panel illustrates computer-generated data. A square pulse identical to that used to drive the iontophoresis of Ca was integrated through a leaky integrator (Eq. 3) with a leak constant $K = 0.035$.

At the end of the current pulse, the Ca concentration returned with an exponential time course to its starting level. The exponential Ca loss from the assembly could be fitted with a single time constant. The average value of the time constant of Ca clearance was 28.5 ± 6.5 s (SD; range, 21–37; $n = 5$).

To analyze the Ca clearance from the measuring compartment of the electrode assembly, we elected to model this compartment as an integrator. In the absence of any leak, the Ca concentration change would simply be the time integral of the current injection. In reality, as shown in Fig. 4, the Ca concentration change was not the integral of the square pulse of current; rather, it reached a steady state value during the course of the current pulse, and then decayed exponentially at the end of the pulse. The time course of the observed Ca concentration change, $\Delta[Ca]_o$, could be described as the integral over time of the iontophoresis current achieved by a leaky integrator with a leak constant, K. Thus,

$$\Delta[Ca]_o(t) = \int \left[i_{Ca}(t) - K \int i_{Ca}(t)dt \right] dt, \qquad (3)$$

where $\Delta[Ca]_o(t)$ is the Ca time course of the Ca concentration increase generated by the iontophoresis of Ca by a current of time course $i(t)$. The analytical solution of Eq. 3 indicates that for a square pulse of current, K is the reciprocal of the time constant of decay of Ca concentration at the end of the pulse. From the decay time constant that we measured, we calculate that K had an average value of 0.035 (range, 0.025–0.048). This value indicates that the seals in the electrode assembly are tight: the measuring compartment loses added Ca at a rate of ~3.5%/s.

We confirmed that the measuring compartment is indeed well described as a leaky integrator by comparing experimental data to the theoretical prediction. The right-hand panel of Fig. 4 illustrates a graphic solution of Eq. 3, with an appropriate value of K. The predicted data match well those measured experimentally and shown in the left-hand panel. In all calculations presented, the leak constant, K, of the measuring compartment was taken to be 0.035.

Ca Efflux from the Rod Outer Segment, $J_e(t)$; Kinetics of Ca Concentration Rise at Light Intensities That Saturate the Photocurrent

To determine the kinetics of the light-dependent Ca efflux from the outer segment, $J_e(t)$, we analyzed the Ca electrode signal generated by light intensities that saturate the photocurrent. While the photocurrent is saturated, the conductance of the outer segment plasma membrane is <10 pS since this membrane contains only light-sensitive channels (Baylor and Lamb, 1982; Baylor and Nunn, 1986; Hestrin and Korenbrot, 1987). During photocurrent saturation, therefore, the Ca influx into the outer segment is negligible [$J_i(t) = 0$] and the kinetics of the Ca electrode signal are determined exclusively by the rate of Ca efflux from the outer segment and the Ca leak from the electrode assembly.

We used an experimental method to determine the kinetics of Ca efflux. We replaced the outer segment in the electrode assembly with the iontophoresis electrode and determined the time course of a Ca injection that generated a Ca concentration change identical to that produced by the outer segment. The iontophoresis electrode is an appropriate physical equivalent to the outer segment under saturating light intensities in that neither is permeable to Ca influx. The equivalence of the iontophoresis electrode to the outer segment, however, is limited. In the case of the iontophoresis electrode, Ca flows toward the Ca electrode from a single position in space, located halfway between the Ca electrode and the tip of the suction electrode. In the case of the outer segment, on the other hand, because the density of the dark current is constant along its length (Baylor et al., 1979), the Ca efflux under bright lights should emerge uniformly along its entire length. This means that there are no Ca concentration gradients along the length of the outer segment and that Ca flows toward the Ca electrode from a single position in space, located at the tip of the outer segment. This limitation, it turns out, is not important in the analysis presented here because when diffusion occurs from a fixed position in space toward an impermeant detector, as is the case in our measurements, the time course of concentration changes measured by the detector faithfully follows the time course of concentration change at the site of origin, but is simply delayed in its onset (Crank, 1975). The delay is given by $t = x^2/2D$, where x is the distance between

the detector and the source and D is the diffusion constant of the diffusing molecule. Therefore, when the Ca electrode signals are identical, the kinetics of Ca injection by the iontophoresis electrode should be the same as the kinetics of Ca injection by the outer segment, except in their latencies.

It was important, then, to demonstrate that Ca flux from the iontophoresis electrode toward the Ca electrode occurs by diffusion without the contribution of other forces, for example, electro-osmosis. To this end, we measured the delay between the onset of Ca injection by the iontophoresis electrode and the rise in Ca concentration detected by the Ca electrode. In experiments in which the tip of the iontophoresis electrode was placed 30 μm away from the Ca electrode,

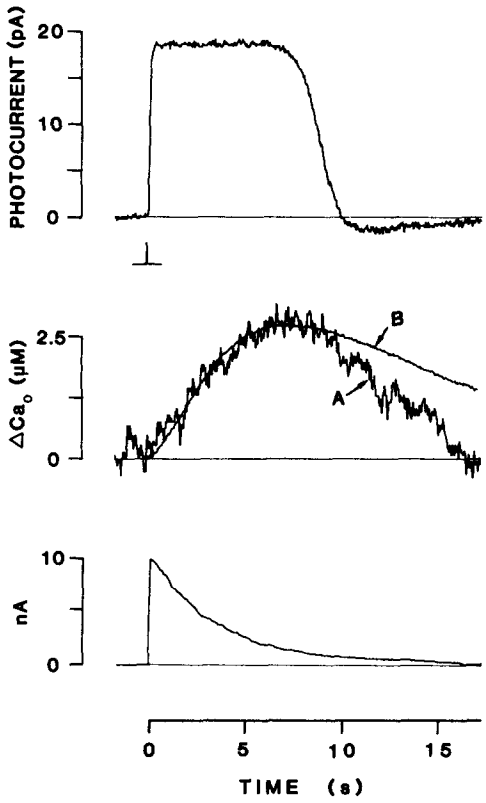

FIGURE 5. Kinetics of light-dependent Ca efflux in response to a flash that saturates the photocurrent. The photocurrent and Ca concentration change generated by a flash that produced 1.8×10^4 Rh* are shown. The top panel illustrates the photocurrent. Trace *A* in the middle panel illustrates the Ca concentration increase. Trace *B* in the middle panel is the Ca concentration change generated in the electrode assembly by the Ca injection illustrated in the bottom panel. The injection rose instantly and then decayed exponentially with a single time constant of 3.5 s. Traces *A* and *B* in the middle panel are nearly identical only while the photocurrent is saturated. The two traces diverge as soon as the photocurrent begins to recover. Once the photocurrent begins to recover, the loss of Ca from the electrode assembly is more rapid in the presence of the outer segment than in the presence of the iontophoretic electrode.

the average latency was 0.425 s. Taking D, the aqueous diffusion constant of free Ca, to be 10^{-5} cm^2/s (R. A. Robinson and Stokes, 1959), the latency calculated from the formula above is 0.45 s. Thus, the kinetics of the Ca electrode signal in response to iontophoretic injections appear to be diffusion limited and therefore the kinetics of Ca flux generated by the iontophoresis electrode should reliably mimic those of the outer segment under bright lights.

Fig. 5 (middle panel) illustrates and compares the Ca signal generated by a rod in response to bright light and that generated by a Ca iontophoretic injection that rose instantly and then decayed exponentially with a single time constant of 3.2 s. The photocurrent simultaneously measured in the rod is illustrated in the

top panel and the bottom panel illustrates the time course of the injected Ca current. Ca iontophoresis generated a Ca concentration change that matched very well the one generated by the cell, but only while the photocurrent was saturated. It is indeed only while the photocurrent is saturated that the iontophoretic Ca injection is expected to match the outer segment Ca injection. The average value of the time constant of exponential decay of the Ca efflux necessary to match the rod signal in all cells studied was 2.5 ± 1.5 s (SD; range, 0.8–6.4; n = 7). Thus, the light-dependent Ca efflux from the rod outer segment, $J_e(t)$, is numerically described as decaying exponentially from an initial value with a single time constant of 2.5 s average value.

Ca Influx into the Rod Outer Segment, $J_i(t)$; Kinetics of Ca Concentration Rise at Light Intensities That Do Not Saturate the Photocurrent

The data in Fig. 5 (middle panel) demonstrate that the Ca electrode signal produced by an exponentially decaying injection of ions differed from the outer segment–generated signal when the photocurrent began to recover from saturation. The Ca signal generated by the outer segment decayed more rapidly than that generated by iontophoresis. This difference reveals that once the photocurrent starts to recover from saturation—that is, the plasma membrane ionic channels begin to reopen—Ca is cleared from the measuring compartment more rapidly than in the absence of this ionic permeability. Thus, once the plasma membrane channels begin to open, the Ca influx into the outer segment is not negligible.

The Ca influx into the outer segment must occur through the light-sensitive channels since these are the only ion channels present in the plasma membrane (Baylor and Lamb, 1982; Baylor and Nunn, 1986; Hestrin and Korenbrot, 1987) and since ion substitution experiments have shown the channels to be permeable to Ca ions (Yau et al., 1981; Hodgkin et al., 1985; Yau and Nakatani, 1985). The kinetics of the Ca influx into the outer segment, $J_i(t)$, should therefore be the same as the kinetics of the photocurrent. If this assertion is correct, knowing the kinetics of the photocurrent allows us to define the kinetics of the Ca influx at all intensities.

A Dynamic Model for the Homeostasis of Cytoplasmic Ca in the Outer Segment

On the basis of the kinetics of the Ca fluxes in and out of the outer segment, we developed a model of the role of the plasma membrane in the control of cytoplasmic Ca in the outer segment and used it to predict the measured light-dependent rise in extracellular Ca. The kinetic model we developed follows a proposition originally made by Yau and Nakatani (1985). The model assumes that in the dark there exists a balance between Ca influx, via the light-sensitive channels, and Ca efflux, via Na/Ca exchangers. Consequently, in the dark, the net Ca flux is zero. Upon illumination, the light-sensitive channels close and the Ca influx therefore decreases, with the same time course as, and to an extent proportional to, the photocurrent. Ca efflux is also assumed to change upon illumination. It is enhanced because light hyperpolarizes the membrane voltage (Brown and Pinto, 1974; Fain, 1976) and because the transport rate of the Na/Ca exchanger is controlled by membrane voltage (Yoshikami, 1985; DiPolo et

al., 1985). Ca efflux also changes upon illumination because the Na/Ca exchanger transport rate is controlled by changes in the cytoplasmic free Ca concentration near the membrane (Schnetkamp, 1980; Requena, 1983; Blaustein, 1984). The model assumes that the changes in the cytoplasmic Ca concentration near the membrane are controlled by the balance between Ca influx and efflux. The contributions of other sources or sinks of Ca to these changes are neglected. In our model, we assumed the Na/Ca exchanger transport rate increases linearly 37% for every 25-mV hyperpolarization, a value recently determined by DiPolo et al. (1985). We estimated the time course of the photovoltage by high-pass-

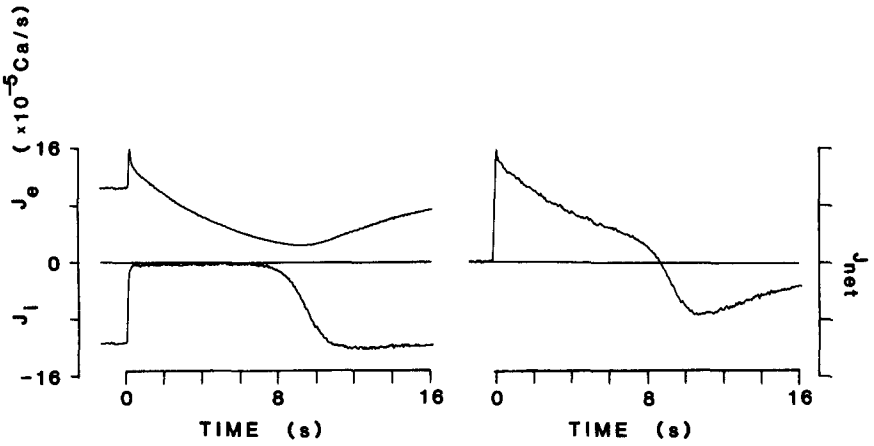

FIGURE 6. Kinetics of Ca influx, Ca efflux, and net flux in response to a flash that saturates the photocurrent amplitude (1.8×10^4 Rh*). The panel on the left illustrates the Ca efflux (upper trace) and Ca influx (lower trace). In the dark, efflux and influx are identical. The magnitude of the dark flux was calculated from the Ca concentration change generated by this cell, as described in the text. After the flash, the influx stops and then recovers with the same time course as the photocurrent. The time course of the change in Ca efflux is calculated continuously by the model discussed in the text. The panel on the right illustrates the net Ca flux, the sum of influx and efflux. This flux is zero in the dark; after the flash, there is a net efflux followed by an influx.

filtering the photocurrent data, as described by Baylor et al. (1984). We also assumed that the exchanger transport rate increased linearly with the cytoplasmic free Ca concentration. This behavior is characteristic of the exchanger in the presence of millimolar levels of ATP (Blaustein, 1984) and the outer segment contains 2–5 mM ATP (W. E. Robinson and Hagins, 1979; Biernbaum and Bownds, 1985; Salceda et al., 1985). With these simple assumptions, we created a dynamic model that enabled us to calculate continuously the Ca influx and efflux of the outer segment and the cytoplasmic and extracellular Ca concentrations as a function of time. The model is detailed fully in the Appendix. It is important to emphasize that the changes in both the cytoplasmic and extracellular Ca concentrations predicted by the model are simple consequences of the difference in the rates of Ca influx and efflux and are not defined independently in the model.

Fig. 6 illustrates the results of calculations executed by the model and based

on the experimentally measured photocurrent and time constant of decay of the Ca efflux. The figure shows the response to a flash that photoexcited 1.8×10^4 rhodopsin molecules in the rod. The panel on the left illustrates the Ca influx, $J_i(t)$, and efflux, $J_e(t)$, while that on the right illustrates their sum, or net Ca flux, $J_{net}(t)$. In the dark, there exists a steady Ca influx, balanced by a steady efflux with a zero net flux. In response to a saturating light stimulus, Ca influx ceases nearly instantly with the time course of the photocurrent. Ca efflux, in contrast,

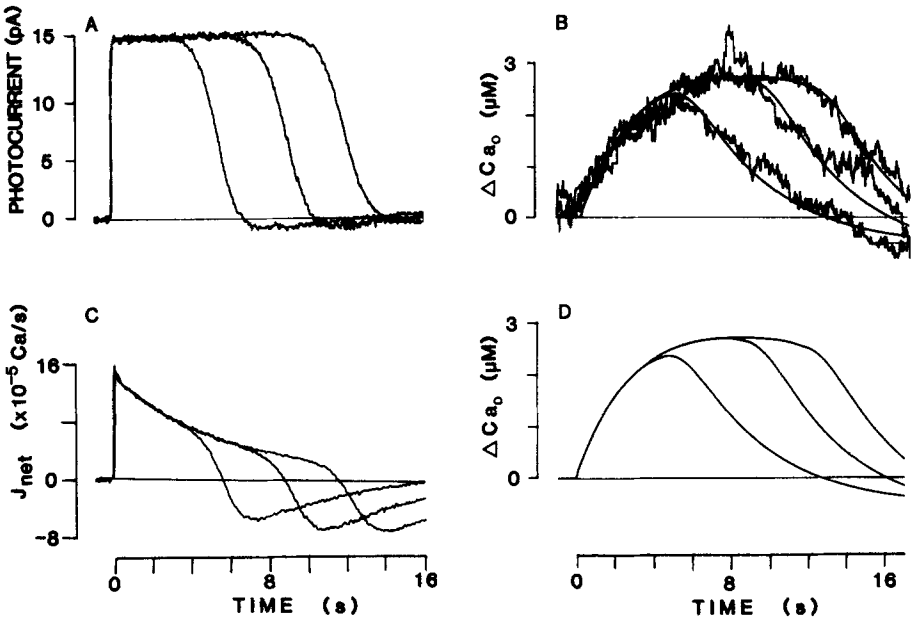

FIGURE 7. Comparison between the measured light-dependent Ca concentration increase and that predicted by the dynamic model. *A* and *B* illustrate photocurrents and Ca concentration changes measured experimentally in a single rod in response to flashes that excited 8.3×10^3, 1.8×10^4, and 7×10^4 rhodopsin molecules. *C* and *D* show data generated by the kinetic model discussed in the text. *C* illustrates the net Ca flux underlying each of the corresponding photocurrents. *D* illustrates the change in extracellular Ca concentration predicted by the model. The predicted concentration changes are essentially identical to those observed experimentally. This is emphasized in *B*, where the experimentally collected data (noisy tracings) are superimposed on the predicted data (smooth tracings).

changes at a slower rate, as defined by the rate of change of the membrane voltage and Ca concentration. The voltage dependence of the exchanger rate gives rise to the initial, transient enhancement seen in the Ca efflux. After this enhancement, the Ca efflux decays toward a value of zero as a single exponential with a time constant of 4.8 s. The decay in the efflux rate reflects primarily the decay in intracellular free Ca. The net Ca flux is outward. As the photocurrent recovers from saturation, both Ca influx and efflux are activated, as shown in the left-hand panel. The influx is activated, of course, because the ionic channels

have reopened; the efflux is activated because the intracellular Ca rises as Ca enters the outer segment. The net flux, the sum of influx and efflux, is transiently inward until the initial, dark condition of zero net flux is reestablished.

We tested the adequacy of the model by using it to predict light-dependent changes in the external Ca concentration and comparing the predictions with experimental results. Fig. 7 illustrates photocurrents (*A*) and Ca concentration changes (*B*) measured in the same cell in response to flashes of increasing intensity, all sufficiently bright to saturate the photocurrent. Panel *C* illustrates the net Ca fluxes from the outer segment that accompany the photocurrents in *A* and have been calculated through the model. To predict the Ca concentration

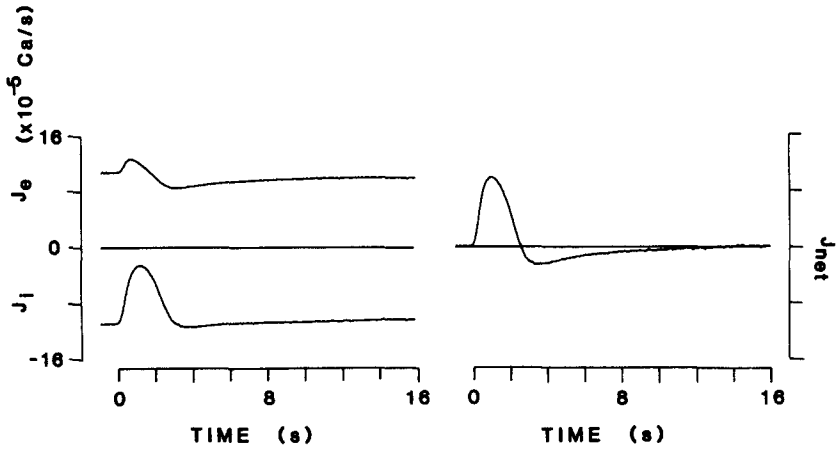

FIGURE 8. Kinetics of Ca influx, Ca efflux, and net flux in response to a flash that does not saturate the photocurrent amplitude (66 Rh*). The panel on the left illustrates the Ca efflux (upper trace) and Ca influx (lower trace). In the dark, influx and efflux are identical. The magnitude of the flux was calculated from the maximum light-dependent Ca concentration change measured for this cell, as described in the text. The time course of the influx is identical to that of the photocurrent generated by the flash. The time course of the efflux is calculated by the model. The panel on the right illustrates the net Ca flux, the sum of influx and efflux. This flux has a starting, dark value of zero; it is first dominated by the efflux of Ca and is then followed by a net influx.

changes generated by the net Ca flux, we integrated this flux with a leaky integrator of the features defined for the electrode assembly (Eq. 3). The predicted Ca concentration changes are illustrated in *D*. Panel *B* illustrates the experimentally recorded data superimposed with the predicted Ca concentration changes. The match between the data and the prediction is excellent. Thus, the model is probably valid and Fig. 7*C* does represent the light-activated net Ca flux at the saturating intensities tested.

We used the model to calculate the Ca efflux, influx, and net flux activated by nonsaturating light intensities. Fig. 8 illustrates the Ca influx, efflux, and net flux observed in response to the photoexcitation of 66 rhodopsin molecules. In the dark, the Ca efflux and influx are, again, steady and identical. In response

to illumination, the influx is transiently reduced with the time course of the photocurrent. The Ca efflux is first activated by the membrane hyperpolarization and then declines as the Ca concentration near the membrane decreases. The net Ca flux is composed of an initial Ca efflux followed by an influx before returning to its dark, zero value.

The model was again tested by its ability to accurately predict the observed Ca concentration changes at various nonsaturating light intensities. Fig. 9 illustrates photocurrents (*A*) and Ca electrode signals (*B*) recorded in a single rod in

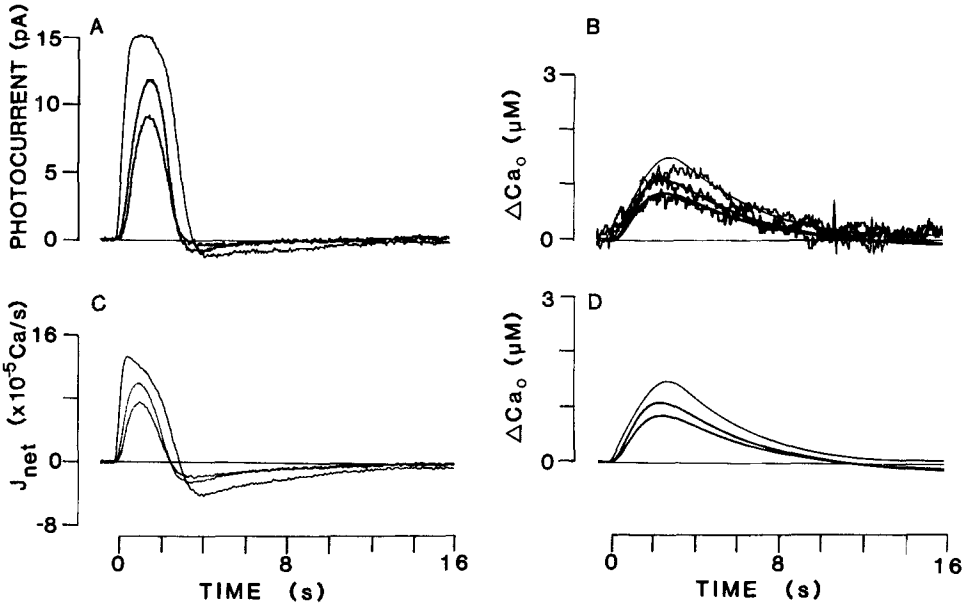

FIGURE 9. Comparison between the measured light-dependent Ca concentration increase and that predicted by the dynamic model. *A* and *B* illustrate photocurrents and Ca concentration changes measured experimentally in a single rod in response to flashes that excited 33, 66, and 275 rhodopsin molecules, respectively. *C* and *D* show data generated by the kinetic model discussed in the text. *C* illustrates the net Ca flux underlying each of the corresponding photocurrents. *D* illustrates the changes in extracellular Ca concentration predicted by the model. The predicted changes are essentially identical to those actually observed. This is emphasized in *B*, where the experimentally collected data (noisy tracings) are superimposed on the predicted data (smooth tracings).

response to stimuli of varying intensities. The net Ca fluxes calculated through the model are also shown (*C*), as well as the Ca concentration changes predicted by leaky integration of the net Ca flux (*D*). The predicted and observed Ca concentration changes are superimposed in *B*. The fit between the predicted and the observed data is excellent.

Dependence of the Amplitude and Rate of the Ca Concentration Change on Light Intensity

The data in Fig. 3 demonstrate that the peak amplitude and the rate of rise of the light-dependent increments in the extracellular Ca concentration are de-

pendent on the stimulus intensity. Fig. 10 illustrates the dependence of the peak amplitude of the Ca signal on light intensity measured in 11 different rods and the dependence on light intensity of the photocurrent peak amplitude. Because individual cells exhibited different maximum peak photocurrent and Na/Ca exchange rates, it was necessary to normalize the individual data points in order to compare the collected data. The photocurrent peak amplitude was normalized for each cell relative to the saturating photocurrent amplitude recorded for that cell. Saturating photocurrents ranged between 12 and 21 pA. The peak amplitude of the Ca concentration change was normalized for each cell relative to its photocurrent peak amplitude and to its Na/Ca exchanger activity. The exchanger

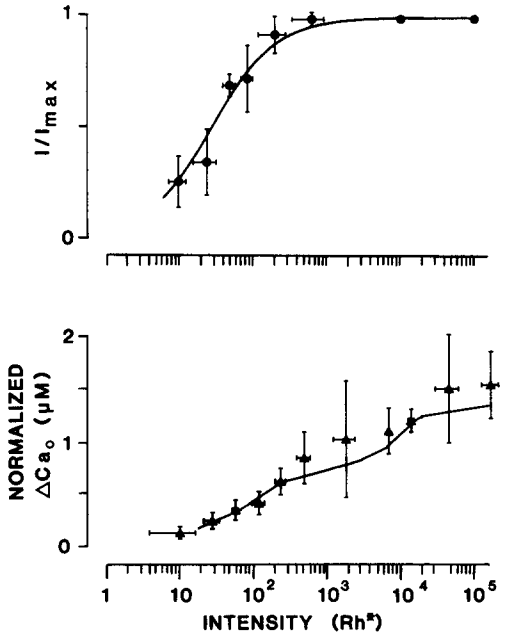

FIGURE 10. Light intensity dependence of the peak amplitude of the photocurrent and of the maximum rise in extracellular Ca concentration change. Data were normalized as described in the text. Data from eight different rods are shown. The continuous line drawn through the photocurrent data is the Michaelis function (Eq. 5) fitted to the data by eye. The continuous lines through the Ca concentration data were generated theoretically by the kinetic model of Ca homeostasis described in the text.

rate for each cell was measured by the time constant of the exponential decay of Ca efflux recorded under current-saturating light stimuli. Thus,

$$[\mathrm{Ca}(E)] = [\mathrm{Ca}(E)]_m(I_{max}/I)(\tau/\tau_{min}), \quad (4)$$

where $[\mathrm{Ca}(E)]_m$ is the peak concentration change measured at intensity E, I is the maximum photocurrent peak amplitude for the cell, I_{max} is the maximum photocurrent recorded for all cells, τ is the time constant of decay of Ca efflux for that cell, and τ_{min} is the minimum value of this constant for all cells.

In Fig. 10, the curve drawn through the photocurrent peak amplitude data (top panel) is a fit to the data of the Michaelis function

$$I(E) = I_{max}E/(E + S), \quad (5)$$

where $I(E)$ is the peak amplitude at intensity E, I_{max} is the saturating amplitude, and S is the intensity at which the photocurrent reaches half-saturation. This function has been repeatedly shown to describe adequately the photocurrent

peak amplitude dependence on light (Fain, 1976; Baylor et al., 1979). The value of S in our data was ~33 bleached rhodopsin molecules. The photocurrent amplitude saturated when ~300 rhodopsin molecules were bleached.

We tested the validity of our dynamic model of Ca homeostasis by using it to predict the dependence of the peak Ca concentration change on light intensity. The continuous line in the bottom panel of Fig. 10 illustrates the function generated by the model. The experimental data lie near the model-predicted values, reinforcing the credibility of the model. The peak Ca concentration change increased with light intensity up to a saturating value at nearly 10^5 Rh*. At low light intensities, up to a few hundred Rh*, the Ca concentration change was, on the average, ~0.01 μM/Rh*, or ~2×10^4 ions/Rh*. The maximum

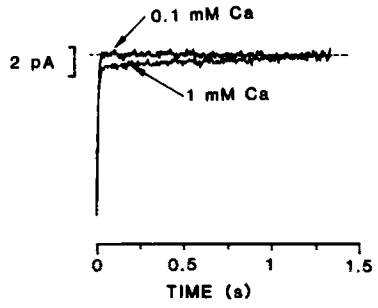

FIGURE 11. Current generated by the electrogenic transport of the Na/Ca exchanger. The figure shows time-expanded photocurrents measured in response to flashes that excited ~2×10^5 rhodopsin molecules in two different rods incubated in L-15 medium containing either 1 mM or 0.1 mM external Ca, as indicated. In the presence of 1 mM Ca, the photocurrent approaches a limiting value with an exponentially decaying component of ~0.7 s time constant and 0.5 pA maximum amplitude. This component has been ascribed to the electrogenic activity of the Na/Ca exchanger (Yau and Nakatani, 1985). This component cannot be reliably resolved from the noise of the signal in 0.1 mM.

extracellular Ca concentration change was, on the average, 4.5 μM, or ~6×10^6 ions. These values are similar to those reported previously (Gold and Korenbrot, 1980, 1981). The initial rate of Ca release increased with light intensity with a dependence similar to that of the photocurrent peak amplitude on light intensity. The initial rate of rise reached a saturating average value of 1.8 μM/s or ~3×10^6 Ca/s at the same intensity that saturates the photocurrent. This is a restatement of the fact presented and analyzed in Fig. 6: the initial Ca efflux is maximal when all the ionic channels close simultaneously.

The Search for an Na/Ca Exchange Current Component in the Photocurrent

Yau and Nakatani (1985) measured an ionic current that they interpreted to arise from the electrogenic activity of the Na/Ca exchanger and found it to decay exponentially with a time constant of 0.4 s after a bright flash. In our experiments, on the other hand, the Ca efflux via the Na/Ca exchanger decays exponentially with an average time constant of 2.5 s after a bright flash. This

difference in values might arise from effects of extracellular Ca concentrations, since our measurements were conducted in 0.1 mM Ca, while those of Yau and Nakatani were carried out in 1.0 mM Ca. To help resolve this discrepancy, we compared the Na/Ca exchanger current recorded at these two external Ca concentrations. Fig. 11 illustrates photocurrents measured at saturating light intensities in two different cells in perfusion medium containing either 0.1 or 1 mM Ca. The electrogenic current of the Na/Ca exchanger is apparent in the presence of 1 mM Ca as the rounded corner in the rising phase of the photocurrent, as Yau and Nakatani have shown. The values for the initial amplitude and the time constant of this electrogenic component varied from cell to cell: mean amplitude, 0.95 pA (range, 0.76–1.2); mean time constant, 0.58 s (range, 0.27–0.74). In contrast, in 0.1 mM external Ca, the Na/Ca electrogenic current was not detectable. This, we believe, is simply because of the limited resolution of the electrical measurement. As presented above, the maximum Ca efflux in 0.1 mM external Ca has an average value of $\sim 3 \times 10^6$ Ca/s. Assuming a 3:1 Na/Ca exchange stoichiometry, as Yau and Nakatani have done, the Ca flux would generate a net influx of positive charge of 3×10^6 charges/s, or ~0.3 pA current. A current of this magnitude is difficult to resolve in the noise of our electrical measurements, but is unmistakably observed with the Ca electrodes. Thus, in 0.1 mM Ca, the electrical measurements underestimate the quantitative characteristics of the Na/Ca exchanger flux.

DISCUSSION

We have simultaneously measured the photocurrent and the light-dependent changes in extracellular Ca in single toad rod photoreceptors. The results of our measurements reveal that the Ca concentration changes arise from light-dependent decrements in both the influx and efflux of Ca across the outer segment plasma membrane. The kinetics of the light-dependent Ca influx are the same as those of the photocurrent. The kinetics of the light-dependent Ca efflux are a function of the membrane voltage and the cytoplasmic Ca concentration. At light levels that saturate the photocurrent amplitude, the Ca efflux has an initially large value that decays exponentially with an average time constant of ~2.5 s. These results are in full agreement with those recently reported by Gold (1986) in the frog retina. Yoshikami et al. (1980) previously showed in the rat retina the superficial similarity of the time course of Ca flux and photocurrent at dim lights. They did not investigate this relationship at bright light levels. Our studies differ technically from those of Gold (1986) and Yoshikami et al. (1980) in one fundamental way: these investigators estimated the kinetics of the net membrane Ca flux through differentiation of the measured extracellular Ca concentration change. They could not resolve the Ca influx and efflux independently. We developed a method that allowed us to resolve the various fluxes that contribute to the observed Ca concentration change.

The first reports on the existence of a light-activated release of Ca by the outer segment (Yoshikami et al., 1980; Gold and Korenbrot, 1980, 1981) interpreted this phenomenon as being consistent with the Ca hypothesis of phototransduction proposed by Hagins (1972), although some inconsistencies were noted (Gold and

Korenbrot, 1981). The findings presented here, and similar results reported by Gold (1986)—in particular, that the light-dependent Ca efflux and the photocurrent have different time courses—are inconsistent with the simplest form of the Ca hypothesis interpretation. Alternative models that preserve the Ca hypothesis and account for the kinetic difference can be developed, as discussed elsewhere (Korenbrot and Miller, 1986; Gold, 1986). However, our results, added to the failure of the hypothesis to predict the effects of intracellular Ca buffers on phototransduction (Korenbrot and Miller, 1986; Lamb et al., 1986; Miller, D. L., and J. I. Korenbrot, manuscript in preparation) and the inability of Ca to control the probability of opening of the light-sensitive channels of the outer segment membrane (Fesenko et al., 1985), suggest that a different hypothesis is necessary to explain the effects of Ca in rod phototransduction and the mechanism of the light-dependent release of Ca.

A Model of a Mechanism to Control the Cytoplasmic Ca Concentration: Dynamic Balance between Ca Efflux and Influx

In the Results, we developed in detail a kinetic model to explain the observed light-dependent Ca concentration changes. The model assumes that there exists in the outer segment a dynamic interplay between Ca influx, via the light-sensitive channels, and its efflux, via the Na/Ca exchanger. The net membrane Ca flux changes upon illumination simply because the rate of change of the Ca influx in response to a flash is quicker than the rate of change of the efflux. The model makes no independent assumptions at all about changes in the cytoplasmic or extracellular Ca concentrations. These two parameters do change, but simply as a passive consequence of the closure of membrane channels in the presence of a continued extrusion of Ca. The time course and amplitude of the Ca concentration changes predicted by the model match well the data collected experimentally at all light intensities tested. Also, the model predicted well the dependence on light intensity of the peak amplitude of the Ca concentration change.

An important point that must be emphasized is that the transport rate of the Na/Ca exchanger is controlled by the free cytoplasmic Ca concentration in the space immediately adjacent to the plasma membrane, where the exchangers are located. This concentration need not be the same throughout the cytoplasmic volume of the outer segment. Indeed, the space-averaged intracellular free Ca concentration in the toad rod outer segment is ~270 nM (Miller and Korenbrot, 1986; Miller, D. L., and J. I. Korenbrot, manuscript in preparation). This corresponds to $\sim 2 \times 10^5$ free Ca ions. However, the total amount of Ca released in response to bright illumination is $\sim 2.5 \times 10^6$, much more than the measured free amount. This observation may reflect the existence near the membrane of a relatively unstirred pool of Ca ions, resulting in a higher Ca activity near the plasma membrane. Recent studies have shown that Ca ions are indeed not distributed uniformly throughout the cytoplasm of some cells (Harary and Brown, 1984; Williams et al., 1985). An alternative explanation is the existence of uniformly distributed Ca-binding sites, which are unloaded as the Ca activity decreases in response to light.

The kinetic model of Ca homeostasis predicts a light-dependent decrease in the cytoplasmic Ca concentration. The time course of this concentration decrease can be predicted by the model, but the predictions can be taken as exact only for the restricted space near the membrane that influences the transport rate of the Na/Ca exchanger. For other points within the cylindrical outer segment, the time course of the concentration change will be nearly the same as that near the membrane, after a delay (Crank, 1975). Fig. 12 depicts a model-generated set of kinetic data that predict the characteristics of the light-dependent decrease in the intracellular Ca concentration associated with the experimental photocur-

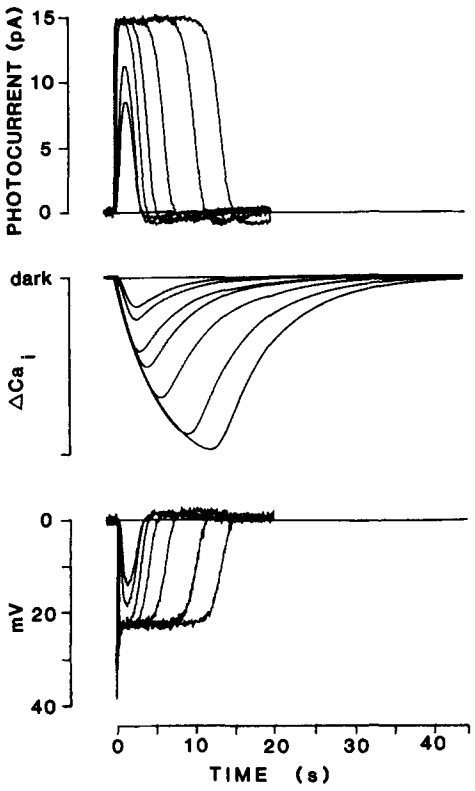

FIGURE 12. Model calculations of the time course of the light-dependent decrease in cytoplasmic free Ca near the plasma membrane. The top panel illustrates photocurrents generated by flashes that excited 33, 66, 275, 8.3×10^3, 1.8×10^4, and 7×10^5 rhodopsin molecules. The middle panel shows the time course and extent of the decrease in cytoplasmic Ca calculated for each photocurrent by the model discussed in the text. The initial, dark Ca concentration cannot be reliably predicted; the limiting concentration in the light, on the other hand, is ~63 nM. The bottom panel illustrates the calculated photovoltages associated with each of the photocurrents.

rents illustrated. Also illustrated are the photovoltages associated with the photocurrents and calculated by the model. The precise amplitude of the Ca concentration decrease cannot be predicted with any confidence because the Ca concentration in the dark in the restricted space near the membrane is unknown. On the other hand, it is possible to predict the lowest Ca concentration observed when the photocurrent remains saturated long enough to allow the Ca efflux to be zero. Under these conditions, the net Ca influx and efflux will be zero and the Na/Ca exchanger will be at thermodynamic equilibrium. At equilibrium (Requena, 1983; Blaustein, 1984):

$$[Ca]_o/[Ca]_i = ([Na]_o/[Na]_i)^3 \exp(-VF/RT). \quad (6)$$

During photocurrent saturation and under our experimental conditions: V_m = −65 mV (Brown and Pinto, 1974), $[Ca]_o$ = 0.1 mM, $[Na]_o$ = 110 mM, and $[Na]_i$ = 22 mM (Somlyo and Walz, 1985). Solving Eq. 6 indicates that the lowest Ca concentration in the outer segment near the membrane should be 63 nM.

A particularly intriguing feature of the predicted changes in the cytoplasmic concentration is that after recovery of photocurrent saturation, cytoplasmic Ca rises at a rate slower than that of the current recovery. Phototransduction processes regulated by this concentration rise might therefore be expected to lag in time behind the recovery of the photocurrent. It is well established that dark adaptation, the recovery of rod photosensitivity that follows the end of steady illumination, is slower than the recovery of the photocurrent (Fain, 1976; Hemila, 1977). Perhaps the rise in cytoplasmic Ca is one of the molecular processes associated with the recovery of rod photosensitivity (dark adaptation), a possibility discussed in detail in another report (Korenbrot and Miller, 1986; Miller, D. L., and J. I. Korenbrot, manuscript in preparation).

An important consequence of the kinetic model of the control of the cytoplasmic Ca concentration is that the concentration changes follow, rather than precede, the closing of the light-sensitive channels. Thus, the role of Ca in phototransduction cannot be that of a messenger linking rhodopsin photoexcitation to channel closure; rather, it is that of a cytoplasmic modulator that provides inertial control on the mechanisms that directly open and/or close the membrane channels.

The role of the plasma membrane in controlling Ca homeostasis, while apparently sufficient to account for the observed changes in the extracellular Ca concentration, should not be taken to be the sole regulator of intracellular Ca. Rod disks contain Ca (Szuts and Cone, 1977) and the metabolic machinery to load it (Puckett et al., 1985). These membranes also contain nonselective cationic channels through which Ca permeates that are apparently controlled by the cyclic GMP cytoplasmic concentration (Caretta and Cavaggioni, 1983; Koch and Kaupp, 1985). Interestingly, the light-dependent decrease in cyclic GMP would decrease the conductance of the disk membranes. In the presence of a continuous pump, this disk membrane mechanism would also lead to a light-dependent decrease in cytoplasmic Ca level. Thus, disk membranes may also play a role in regulating cytoplasmic Ca levels, a proposition that cannot now be dismissed.

The Contribution of Ca to the Dark Current

Our measurements of extracellular Ca concentration have confirmed the conclusion of ion substitution experiments that the light-sensitive channels are permeable to Ca. The fraction of the dark current carried by Ca in the presence of 0.1 mM extracellular Ca can be calculated from our data by two independent means. The first one involves the presumption, defined in the kinetic model, that the dark Ca influx is the same as the dark Ca efflux. The magnitude of the standing, dark Ca efflux can be calculated from the Ca electrode data. The maximum measured light-dependent Ca concentration change is the time integral of the Ca efflux. Since this efflux has an exponential time course, it can be shown that

$$J_{max} = [Ca]_{max}/\tau, \quad (7)$$

where J_{max} is the peak efflux rate, $[Ca]_{max}$ is the maximum light-dependent Ca concentration change, and τ is the time constant of decay of the Ca efflux. From the peak Ca efflux measured in 11 cells, the Ca efflux in the dark was found to be 1.37 ± 0.7 μM/s (SD). Considering the volume of the measuring compartment of the electrode assembly, 2.7 pl, the Ca efflux rate in the dark can be calculated to be 2.2×10^6 ions/s, or a current of 0.34 pA. For an average dark current of 18 pA, this represents ~1.9% of the dark current. The second method is based on the direct measurement of Ca influx at the moment the ion channels begin to open after photocurrent saturation. The Ca influx was measured from data such as those shown in Fig. 6. These measurements reveal that Ca ions carry ~1.8% of the dark current on the average. Our two independent measurements agree closely. These values, however, are smaller than the 10–15% estimated by Yau and Nakatani (1985) and Gold (1986) in the presence of 1 mM extracellular Ca. The difference may be explained by the simple proposition that the fraction of the dark current carried by Ca depends on the external Ca concentration.

While our kinetic model predicts results consistent with the experimental data, it may not be the only model able to describe the Ca fluxes across the rod outer segment membrane. It is the simplicity of the model, the absence of ad hoc assumptions, and the fact that it is based on well-grounded experimental observations that make it attractive. The molecular role of a light-induced decrease in Ca activity in the outer segment cytoplasm has yet to be defined precisely. We have argued (Korenbrot and Miller, 1986; Miller, D. L., and J. I. Korenbrot, manuscript in preparation) that intracellular Ca is important in controlling the kinetics and gain of the photocurrent, perhaps by regulating the lifetime of the excitatory transmitter in phototransduction.

APPENDIX

Model of Ca Fluxes across the Outer Segment Plasma Membrane

Assume that in the dark the Ca influx, J_i, and the Ca efflux, J_e, are time independent and have the same value. We define the efflux as positive. The net flux in the dark, J_{net}, is zero.

$$^dJ_e = -^dJ_i;$$

$$^dJ_{net} = {}^dJ_i + {}^dJ_e = 0.$$

Assume that the Ca influx occurs through the light-sensitive channels. therefore, the Ca influx in the light, $^lJ_i(t)$, decreases to an extent proportional to and with the same time as the photocurrent, $I_{ph}(t)$. The experimentally recorded photocurrents are provided as data to the model:

$$^lJ_i(t) = {}^dJ_i + \alpha I_{ph}(t).$$

Assume that the Ca efflux occurs through Na/Ca exchangers. Therefore, the Ca efflux in the light, $^lJ_e(t)$, changes as a function of the changes in membrane voltage, $\Delta V_m(t)$, and in the cytoplasmic Ca activity, $\Delta[Ca]_i(t)$ (Requena, 1983). The Na/Ca transport rate is assumed to increase 37% for every 25 mV of hyperpolarization (DiPolo et al., 1985). The time course of the membrane hyperpolarization was calculated from the photocurrent data using the economy model of Baylor et al. (1984). Hyperpolarization was defined as negative voltage:

$$dV_m/dt = (1/g_\infty)dI_{ph}/dt + I_{ph}/(g_o\tau_L) - (1/\tau_L)V_m(t),$$

with $g_\infty = 2.5 \times 10^{-10}$ S, $g_o = 7.3 \times 10^{-10}$ S, and $\tau_L = 0.045$ s.

$$^1J_e(t) = \{^dJ_e(t) + \beta\Delta[Ca]_i(t)\}[1 - (0.37/25\text{ mV})\Delta V_m(t)].$$

β is a constant defined by the transport rate of the Na/Ca exchanger. The value of β was determined experimentally for each rod and is the reciprocal of the time constant of the exponential decay of Ca efflux observed in response to saturating light intensities. We determined the value of β by comparing the kinetics of Ca concentration changes produced by the outer segment with those produced by an exponentially decaying iontophoretic injection of Ca (see Fig. 5). The time constant of the exponential injection was varied until a value was found that generated a Ca signal that matched that generated by the outer segment. β was calculated from this time constant.

Changes in the cytoplasmic free Ca concentration near the membrane are assumed to result from changes in the net Ca flux across the membrane. The contributions of intracellular sources or sinks of Ca are neglected. The Ca concentration changes are calculated by integration of the net Ca flux in the light, $J_{net}(t)$. The transport activity of the Na/Ca exchanger is assumed to be proportional to the cytoplasmic Ca concentration (Blaustein, 1984):

$$\Delta[Ca]_i(t) = -\int {}^1J_{net}(t)dt;$$

$$^1J_{net}(t) = {}^1J_i(t) + {}^1J_e(t).$$

The Ca concentration change measured outside the rod is given by the time integral of the net Ca flux across the outer segment membrane, corrected for the leak of the measuring compartment of the electrode assembly,

$$\Delta[Ca]_o(t) = \int\left[{}^1J_{net}(t) - K\int {}^1J_{net}(t)dt\right]dt,$$

where K is the leak rate of the electrode assembly, determined experimentally to be 0.035 (see Fig. 4). These equations were solved simultaneously with numerical methods.

We thank Drs. E. Phillips, D. Bolnick, D. Copenhagen, and R. Fernald for their invaluable comments on the manuscript.

This work was supported by National Institutes of Health grant EY-01586.

Original version received 25 August 1986 and accepted version received 10 February 1987.

REFERENCES

Amman, D., R. Bissig, M. Gueggi, E. Pretsch, W. Simon, I. J. Borowitz, and L. Weiss. 1975. Preparation of neutral ionophores for alkali and alkaline earth cations and their application. *Helvetica Chimica Acta.* 58:1535–1548.

Bader, C. R., D. Bertrand, and E. A. Schwartz. 1982. Voltage-activated and Ca-activated current studied in solitary rod inner segments from the salamander retina. *Journal of Physiology.* 331:253–284.

Baylor, D. A., and T. D. Lamb. 1982. Local effects of bleaching in retinal rods of the toad. *Journal of Physiology.* 328:49–71.

Baylor, D. A., T. D. Lamb, and K.-W. Yau. 1979. The membrane current of single rod outer segments. *Journal of Physiology.* 288:589–611.

Baylor, D. A., G. Matthews, and B. J. Nunn. 1984. Location and function of voltage-sensitive conductances in retinal rods of the salamander *Ambystoma tigrinum*. *Journal of Physiology*. 354:203–223.

Baylor, D. A., and B. J. Nunn. 1986. Electrical properties of the light-sensitive conductance of rods of the salamander *Ambystoma tigrinum*. *Journal of Physiology*. 371:115–145.

Biernbaum, M. S., and M. D. Bownds. 1985. Light-induced changes in GTP and ATP in frog rod photoreceptors. *Journal of General Physiology*. 85:107–121.

Blaustein, M. P. 1984. The energetics and kinetics of the Na/Ca exchange in barnacle muscles, squid axons and mammalian heart: the role of ATP. *In* Electrogenic Transport. M. P. Blaustein and M. Lieberman, editors. Raven Press, New York. 404 pp.

Bodoia, R. D., and P. B. Detwiler. 1985. Patch-clamping recordings of the light-sensitive dark noise in retinal rods from the lizard and frog. *Journal of Physiology*. 367:183–216.

Brown, J. E., and L. H. Pinto. 1974. Ionic mechanism for the photoreceptor potential of the retina of *Bufo marinus*. *Journal of Physiology*. 236:575–591.

Caretta, A., and A. Cavaggioni. 1983. Fast ionic flux activated by cGMP in the membrane of cattle rod outer segment. *European Journal of Biochemistry*. 132:1–8.

Cobbs, W. H., and E. N. Pugh. 1985. Cyclic GMP can increase rod outer segment light sensitive current 10 fold without delay of excitation. *Nature*. 313:585–587.

Crank, J. 1975. The Mathematics of Diffusion. Clarendon Press, Oxford. 414 pp.

Dartnall, H. J. A. 1972. Photosensitivity. *In* Photochemistry of Vision. H. J. A. Dartnall, editor. Springer-Verlag, New York. 122–145.

DiPolo, R., F. Bezanilla, C. Caputo, and H. Rojas. 1985. Voltage dependence of the Na/Ca exchange in voltage-clamped, dialyzed squid axons. *Journal of General Physiology*. 86:457–478.

Fain, G. L. 1976. Sensitivity of toad rods: dependence on wavelength and background illumination. *Journal of Physiology*. 261:71–101.

Fesenko, E. E., S. S. Kolesnikov, and A. L. Lyubarsky. 1985. Induction by cyclic GMP of cationic conductance in plasma membrane of retinal rod outer segment. *Nature*. 313:310–313.

Gold, G. H. 1986. Plasma membrane calcium fluxes in intact rods are inconsistent with the "Ca-hypothesis." *Proceedings of the National Academy of Sciences*. 83:1150–1154.

Gold, G. H., and J. I. Korenbrot. 1980. Light-induced Ca release by intact retinal rods. *Proceedings of the National Academy of Sciences*. 77:5557–5561.

Gold, G. H., and J. I. Korenbrot. 1981. The regulation of Ca in intact retinal rods: a study of light-induced calcium release by the outer segment. *Current Topics in Membranes and Transport*. 15:307–328.

Hagins, W. A. 1972. The visual process: excitatory mechanisms in the primary receptor cells. *Annual Review of Biophysics and Bioengineering*. 1:131–158.

Hagins, W. A., R. D. Penn, and S. Yoshikami. 1970. Dark current and photocurrent in retinal rods. *Biophysical Journal*. 10:380–412.

Harary, H. H., and J. E. Brown. 1985. Spatially nonuniform changes in intracellular calcium ion concentration. *Science*. 224:292–294.

Hârosi, F. I. 1975. Absorption spectra and linear dichroism of some amphibian photoreceptors. *Journal of General Physiology*. 66:357–382.

Haynes, L. W., A. R. Kay, and K.-W. Yau. 1986. Single cGMP-activated channel activity in excised patches of rod outer segment membranes. *Nature*. 321:66–70.

Hemila, S. 1977. Background adaptation in the rods of the frog's retina. *Journal of Physiology*. 265:721–741.

Hestrin, S., and J. I. Korenbrot. 1987. Effects of cyclic GMP on the kinetics of the photocurrent in rods and in detached rod outer segments. *Journal of General Physiology.* In press.

Hodgkin, A. L., P. A. McNaughton, and B. J. Nunn. 1985. The ionic selectivity and calcium dependence of the light-sensitive pathway in toad rods. *Journal of Physiology.* 358:447–468.

Koch, K.-W., and U. B. Kaupp. 1985. Cyclic GMP directly regulates a cation conductance in membranes of bovine rods by a cooperative mechanism. *Journal of Biological Chemistry.* 260:6788–6800.

Korenbrot, J. I., and D. L. Miller. 1986. Calcium ions act as modulators of intracellular information flow in retinal rod phototransduction. *Neuroscience Research.* 4:S11–S34.

Korenbrot, J. I., D. L. Ochs, J. Williams, D. L. Miller, and J. E. Brown. 1986. The use of tetracarboxylate indicators in the measure and control of cytoplasmic calcium. *In* Optical Methods in Cell Physiology. P. De Weer and B. M. Salzberg, editors. John Wiley & Sons, New York. 347–363.

Korn, G. A., and J. V. Wait. 1978. Digital Continuous System Simulation. Prentice Hall, New York.

Lamb, T. D., H. R. Matthews, and V. Torre. 1986. Incorporation of calcium buffers into salamander retinal rods: a rejection of the Ca hypothesis of phototransduction. *Journal of Physiology.* 372:315–340.

MacLeish, P. R., E. A. Schwartz, and M. Tachibana. 1984. Control of the generator current in solitary rods of the *Ambystoma tigrinum* retina. *Journal of Physiology.* 348:645–664.

Matthews, H. R., V. Torre, and T. D. Lamb. 1985. Effects on the photoresponse of calcium buffers and cyclic GMP incorporated into the cytoplasm of retinal rods. *Nature.* 313:582–586.

Miller, D. L. 1986. The role of Ca in retinal rod phototransduction. Ph.D. thesis. University of California at Berkeley. 105 pp.

Miller, D. L., and J. I. Korenbrot. 1986. Effects of the intracellular buffer quin-2 on the photocurrent responses of toad rods. *Biophysical Journal.* 49:281*a*. (Abstr.)

Penn, R. D., and W. A. Hagins. 1972. Kinetics of photocurrent of retinal rods. *Biophysical Journal.* 12:1073–1094.

Puckett, K. L., E. T. Aronson, and S. M. Goldin. 1985. ATP-dependent Ca uptake associated with a disk membrane fraction isolated from bovine retinal rod outer segments. *Biochemistry.* 24:390–400.

Requena, J. 1983. Ca transport and regulation in nerve fibers. *Annual Review of Biophysics and Bioengineering.* 12:237–257.

Robinson, R. A., and R. H. Stokes. 1959. Electrolyte Solutions. Butterworth Press, London. 559 pp.

Robinson, W. E., and W. A. Hagins. 1979. GTP hydrolysis in intact retinal rod outer segments and the transmitter cycle in visual excitation. *Nature.* 280:398–400.

Ruzicka, J., E. H. Hansen, and J. C. Tjell. 1973. Ca selectrode employing a new ion exchanger in a non porous membrane and a solid state reference system. *Analytica Chimica Acta.* 67:155–178.

Salceda, R., G. R. E. M. Van Roosmeen, P. A. A. Jansen, S. L. Bonting, and F. J. M. Daemen. 1985. Nucleotide content of isolated bovine rod outer segments. *Vision Research.* 22:1469–1474.

Schnetkamp, P. P. M. 1980. Ion selectivity of the cation transport system of isolated intact cattle rod outer segments. *Biochimica et Biophysica Acta.* 598:66–90.

Somlyo, A. P., and B. Walls. 1985. Elemental distribution in *Rana pipiens* retinal rods: quantitative electron-probe analysis. *Journal of Physiology.* 358:183–195.

Szuts, E. Z., and R. A. Cone. 1977. Calcium content of rod outer segments and discs. *Biochimica et Biophysica Acta.* 468:194–205.

Williams, D. A., K. E. Fogarty, R. Y. Tsien, and F. S. Fay. 1985. Calcium gradient in smooth muscle cells revealed by the digital imaging microscope using Fura-2. *Nature.* 318:558–561.

Yau, K.-W., P. A. McNaughton, and A. L. Hodgkin. 1981. Effect of ions on the light-sensitive current in retinal rods. *Nature.* 292:502–505.

Yau, K.-W., and K. Nakatani. 1984. Cation selectivity of light-sensitive conductance in retinal rods. *Nature.* 309:352–354.

Yau, K.-W., and K. Nakatani. 1985. Light-induced reduction of cytoplasmic free calcium in retinal rod outer segment. *Nature.* 313:579–582.

Yoshikami, S. 1985. Calcium extrusion by retinal rods modifies light-sensitivity of dark current. *In* Calcium in Biological Systems. R. P. Reuben, G. P. Weiss, and J. W. Putney, Jr., editors. Plenum Publishing Corp., New York. 737 pp.

Yoshikami, S., J. S. George, and W. A. Hagins. 1980. Light-induced calcium fluxes from outer segment layer of vertebrate retinas. *Nature.* 286:395–398.

Zimmerman, A. L., and D. A. Baylor. 1986. Cyclic GMP-sensitive conductance of retinal rods consists of aqueous pores. *Nature.* 321:70–72.